Lawrence Berkeley National Laboratory

Title
Enabling Lithium Metal Anode in Nonflammable Phosphate Electrolyte with Electrochemically Induced Chemical Reactions.

Permalink

Journal

ISSN

Authors
Zhang, Haochuan
Luo, Jingru
Qi, Miao
et al.

Publication Date

DOI

Enabling Lithium Metal Anode in Nonflammable Phosphate Electrolyte with Electrochemically Induced Chemical Reactions

Haochuan Zhang+, Jingru Luo+, Miao Qi, Shiru Lin, Qi Dong, Haoyi Li, Nicholas Dulock, Christopher Povinelli, Nicholas Wong, Wei Fan, Junwei Lucas Bao, and Dunwei Wang*

Abstract: *Lithium metal anode holds great promises for next-generation battery technologies but is notoriously difficult to work with. The key to solving this challenge is believed to lie in the ability of forming stable solid-electrolyte interphase (SEI) layers. To further address potential safety issues, it is critical to achieve this goal in nonflammable electrolytes. Building upon previous successes in forming stable SEI in conventional carbonate-based electrolytes, here we report that reversible Li stripping/plating could be realized in triethyl phosphate (TEP), a known flame retardant. The critical enabling factor of our approach was the introduction of oxygen, which upon electrochemical reduction induces the initial decomposition of TEP and produces Li_3PO_4 and poly-phosphates. Importantly, the reaction was self-limiting, and the resulting material regulated Li plating by limiting dendrite formation. In effect, we obtained a functional SEI on Li metal in a nonflammable electrolyte. When tested in a symmetric Li ‖ Li cell, more than 300 cycles of stripping/plating were measured at a current density of $0.5\ mA\ cm^{-2}$. Prototypical $Li\text{-}O_2$ and Li-ion batteries were also fabricated and tested to further support the effectiveness of this strategy. The mechanism by which the SEI forms was studied by density functional theory (DFT), and the predictions were corroborated by the successful detection of the intermediates and products.*

Introduction

Safety is of paramount importance to modern electrochemical energy storage devices.[1,2] For state-of-the-art Li-ion batteries, a common failure mechanism is understood to start with uneven plating of Li on the anode, leading to the formation of dendrites that could eventually short the circuit.[3–6] The flammable nature of the common electrolytes exacerbates the problem and, hence, the often-dramatic fashion in which batteries fail. The problem of uncontrolled Li plating is especially acute for high capacity electrodes such as Li metal.[7] This is because the reactions between Li metal and the commonly used carbonate-based electrolytes do not produce stable solid-electrolyte interphase (SEI) layers that are critical to safe battery operations.[8–10] How to enable the utilization of Li metal, which features low electrochemical potential and unparalleled capacity, as a direct anode material constitutes a grand challenge in today's intense research on battery technologies.[11–13] Inspired by how SEI enables graphite as a successful anode for Li-ion batteries, researchers have tested a number of approaches on forming a similar SEI on Li metal. For instance, fluoroethylene carbonate (FEC) and $LiNO_3$ have proven effective as additives in introducing LiF-rich and Li_3N/LiN_xO_y-rich SEI, respectively, for stable Li operations.[14–18] A coating of reactive polymer composites has been shown to enable the formation of self-repairing SEI for high-efficiency cycling in lean electrolyte conditions.[19] High-concentration electrolytes have also been demonstrated to significantly change solvation structures and facilitate the formation of a salt-derived SEI, which could help to mitigate anode and electrolyte degradation during extended cycling.[20–23] These exciting progresses notwithstanding, prior demonstrations were carried out in electrolytes that are flammable. The safety concerns connected to the flammability of the electrolyte remain outstanding. It is, therefore, important to explore Li/electrolyte reactions in nonflammable electrolytes. Our work is conceived within this context, with the goal of enabling the formation of a stable SEI to permit operations of Li metal in nonflammable media.

Indeed, great attention has already been attracted to replicate stable SEI formation on Li anode in nonflammable electrolytes.[24,25] With all other parameters equal, being able to replace flammable electrolytes with nonflammable ones should readily improve the safety of batteries. Guided by this idea, a number of solvents have been tested, and organic phosphates (e.g., triethyl phosphate or TEP) stand out.[26,27] This is because the P atoms can act as trapping agents for hydrogen radicals that play critical roles in initiating combustion chain reactions.[26] Prior studies have shown that TEP could serve as a flame retardant to reduce the flammability of conventional electrolytes. Direct utilization of TEP for Li-ion batteries, however, exhibited a multitude of problems, including speculated TEP insertion into graphite and rapidly increasing interface resistance on Li metal.[28,29] To circumvent these issues, approaches such as adding nitrate salts or relying on the decomposition of salts but not solvents have been proposed and proven promising.[20,21,30,31] Inspired by these prior efforts, we hereby report a radically new approach. Our

[*] H. Zhang,[+] Dr. J. Luo,[+] Dr. M. Qi, Dr. S. Lin, Dr. Q. Dong, Dr. H. Li,
N. Dulock, C. Povinelli, N. Wong, Prof. J. L. Bao, Prof. D. Wang
Department of Chemistry, Boston College
2609 Beacon St., Chestnut Hill, MA 02467 (USA)
E-mail: dwang@bc.edu
Prof. W. Fan
Department of Chemical Engineering, University of Massachusetts
686 North Pleasant Street, Amherst, MA 01003 (USA)

[+] These authors contributed equally to this work.

Supporting information and the ORCID identification number(s) for the author(s) of this article can be found under:
https://doi.org/10.1002/anie.202103909.

strategy involves promoting new chemical reaction pathways. It takes advantage of the unique reactivity between electrochemically reduced O_2 species and TEP, which enables the formation of a stable and effective SEI directly on Li anode. The reaction mechanism is supported by density functional theory (DFT) calculations, which are corroborated by the detection of corresponding products both in the electrolyte and in the SEI. When tested in a symmetric Li‖Li cell, >300 cycles of repeated Li stripping and plating was achieved at a current density of 0.5 mA cm^{-2}; when tested in a Li-O_2 prototypical cell, the system showed comparable performance as in a flammable, ether-based electrolyte. A similar strategy worked equally well for prototypical Li-ion batteries. The approach represents a new direction in addressing the critical safety concerns for high-capacity electrochemical energy storage technologies.

Results and Discussion

Our first task was to establish a baseline of TEP electrochemical behaviors when Li is used as an electrode. For this purpose, we prepared 1 M Li bis(trifluoromethanesulfonyl)imide (LiTFSI) in TEP as an electrolyte and constructed a two-electrode Li‖Cu cell that is typically used in the literature for similar studies. In this configuration, Cu served as the working electrode, and Li was used as both the counter and reference electrodes. As shown in Figure 1a, three reduction peaks were observed at ca. 1.4 V, 1.2 V and 0.5 V

(vs. Li$^+$/Li, unless noted, all potentials hereafter are relative to this reference) in the first cycle of cyclic voltammetry (CV) scan. Of them, the peak at 1.2 V was ascribed to the reduction of TEP;[26] the peaks at 1.4 V and 0.5 V may report on the reduction of TEP or TFSI$^-$ (Figures S1,2 in the Supporting Information, SI). The dominating reduction wave past 0 V is due to Li plating onto the Cu working electrode. On the reverse scan, an oxidation peak at ca. 0.1 V was observed, corresponding to the stripping of the newly plated Li. The broad peak at >1.0 V is believed to be due to re-oxidation of SEI components.[32] Notably, these redox features were quickly suppressed upon repeated CV scans, and they were barely visible after 5 cycles (Figure 1b). This feature suggests that the Li stripping/plating in TEP-based electrolyte as observed in the initial CV scan is highly irreversible. Correspondingly, when tested in a symmetric Li‖Li cell, the system exhibited a rapid increase of the stripping and plating overpotentials (Figure 1c). By the 5th cycle, the plating overpotential already reached −0.75 V, and the stripping overpotential reached 1 V. At this point, we considered the test cell has failed. The phenomenon as reported here is consistent with prior reports on TEP electrochemical behaviors when used directly for Li stripping and plating studies.[21,30] It highlights the challenges of using TEP as a non-flammable electrolyte for safe operations of Li electrodes.

Next, we introduced O_2 to the system and observed dramatic improvements. As shown in Figure 1a, the first difference we noticed was the appearance of a new, broad reduction peak at ca. 1.8 V in the Li‖Cu cell in the presence
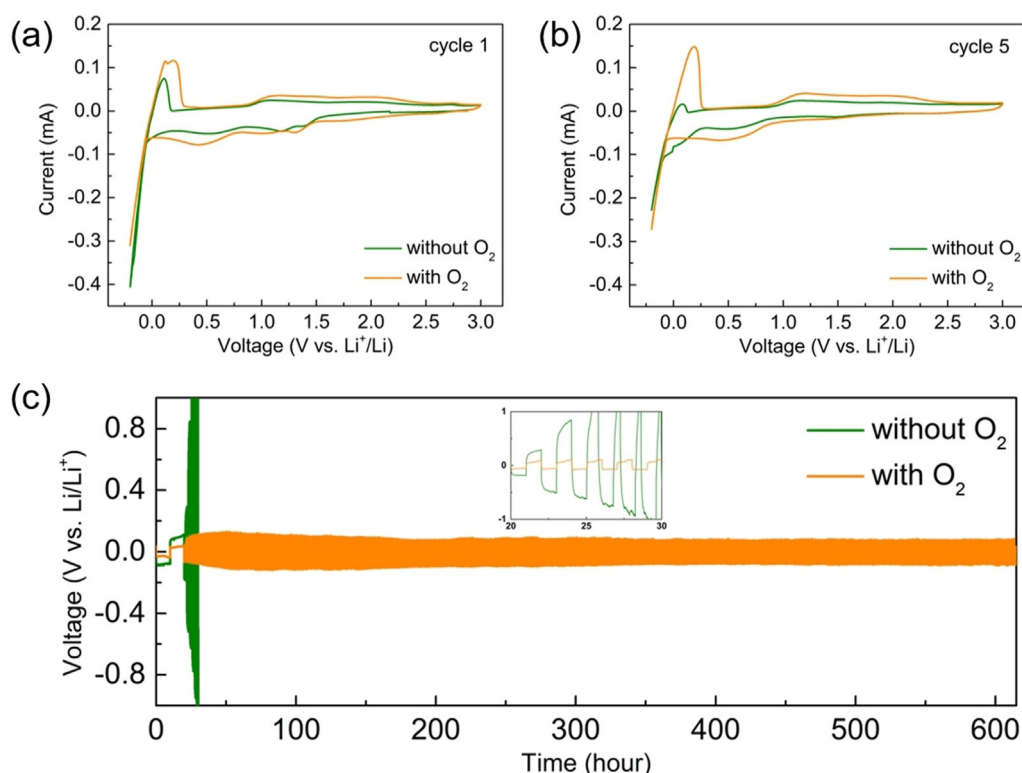

Figure 1. Electrochemical performance of TEP electrolyte with or without O_2. Cyclic voltagram studies of Li‖Cu cell at a scan rate of 0.4 mVs^{-1} in a) first cycle and b) fifth cycle; c) Voltage profiles of Li‖Li cell for long-term cycling test at a current density of 0.5 mA cm^{-2} with 0.5 mAh capacity (forming cycle at a current density of 0.1 mA cm^{-2} with 1 mAh capacity).

of O_2. Presumably, this peak corresponded to the reduction of O_2. While the other reduction features of the first scan were similar to those without O_2, the oxidation peak was indeed more pronounced upon the first reverse scan, reporting a greater recovery of plated Li (ca. 68%) when tested in O_2 than without O_2 (ca. 55%). The most striking difference, however, was how the cell behaved upon repeated CV scans. The Li stripping and plating features were by and large preserved at the 5th cycle (Figure 1b), although the broad peak corresponding to O_2 reduction was now absent. Arguably, the Li stripping peak appeared to be enhanced in comparison to that in the first cycle. These observations led us to conclude that the initial (electrochemical) reactions on the surface of Cu working electrode in O_2-containing TEP electrolyte have resulted in an SEI that favors subsequent Li stripping and plating. To further test this understanding, we next performed cycling tests in a symmetric Li∥Li cell. At a current density of 0.5 mA cm^{-2}, no apparent increase of the overpotentials ($<$120 mV) for both stripping and plating of Li was observed after 300 cycles (Figure 1c), at which point the experiment was artificially terminated. Similar results were reproduced for two more times. Afterwards, following literature proposed method,[33] we conducted cycling test in the Li∥Cu cell to further evaluate the performance of TEP electrolyte. An average Coulombic Efficiency (CE) of 97.4% was achieved in the O_2-containing TEP electrolyte, whereas the Li stripping and plating did not work reversibly in TEP electrolyte without O_2 (Figure S3,4). We are mindful that there is room for further improvement for the unoptimized CE when compared with recently reported electrolyte systems,[25] but the cycling performance obtained here is comparable to the best reported in nonflammable electrolyte systems.[21,30,31] By further exploring the combination of O_2 and other electrolyte additives, we envision that the electrochemical performance of our system could be further improved in the future. It is worth noting that the O_2-induced SEI protection continues to work in fresh electrolytes without

the presence of O_2 (Figure S5), supporting that our method is promising for potential practical systems.

How the simple addition of O_2 greatly improves the Li stripping and platting behaviors in TEP-based electrolyte is not only exciting but also intriguing because the effect of O_2 crossover on Li anode is generally considered one key issue in Li-O_2 batteries.[34] To understand the results, we examined the structure of the Cu electrode after the initial plating of Li by scanning electron microscope (SEM). As shown in Figure 2, with the presence of O_2, a relatively uniform and compact layer of Li with granular microstructures was observed. The grain size was up to 5 μm in diameters. Such morphology resembles those reported in the literature when high-concentration electrolytes were used.[21,35] Recent studies have alluded that a desired structure of electrochemically plated Li should retain an even microstructure with large granular sizes and minimum tortuosity; otherwise the loss of "dead" Li would be significant and, hence, low CE.[36] That we observed such structures by simply adding O_2 to the TEP electrolyte is highly encouraging. In stark contrast, a layer of loose and spikey Li was observed in TEP without O_2, which are typical for Li plating without proper protections of an SEI. Inspired by the prior reports, we hypothesize that the introduction of O_2 has dramatically changed the SEI formation in TEP.

As shown in Figure 3a, the presence of O_2 may lead to at least 3 possible reactions on the anode surface: (i) promoted decomposition of TFSI$^-$ anions by reactive O_2 species; (ii) formation of Li_2O on the anode surface; and (iii) electrochemically induced chemical reactions between TEP solvent and reactive O_2 species. These considerations are made with the assumption that electrochemical reduction of O_2 precedes these surface chemical reactions, which is supported by the broad O_2 reduction peak in the CV scan (Figure 1a). Next, we examined the first possibility that concerns anion decomposition. Recently, there has been a surge of publications on using high-concentration electrolytes, especially FSI$^-$/TFSI$^-$-containing ones, to enable reversible Li metal stripping/
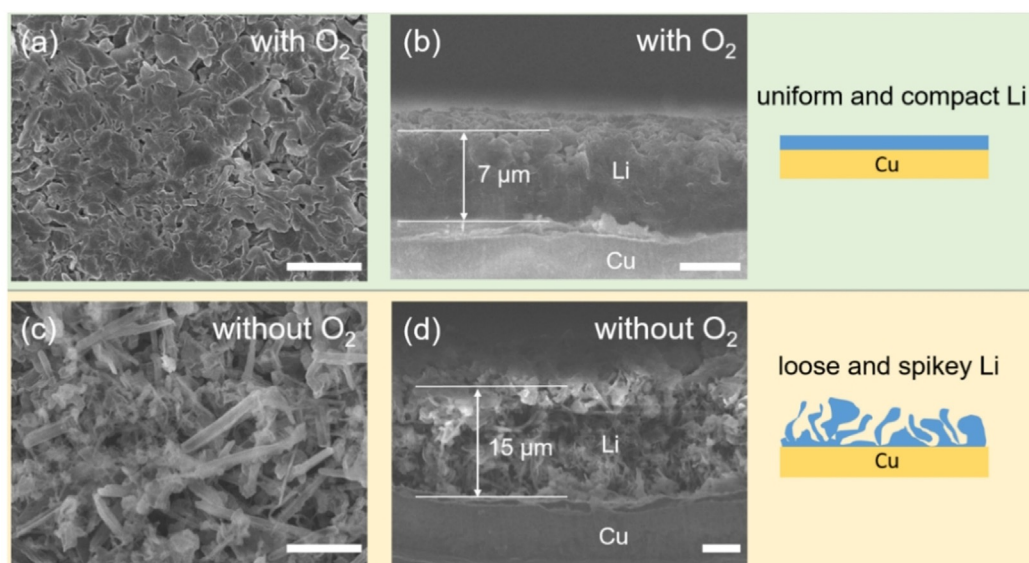
Figure 2. Morphology of deposited Li on Cu electrode surface. SEM images of Li plated electrodes ab) with O_2 and cd) without O_2 in the cell (scale bar: 5 μm).
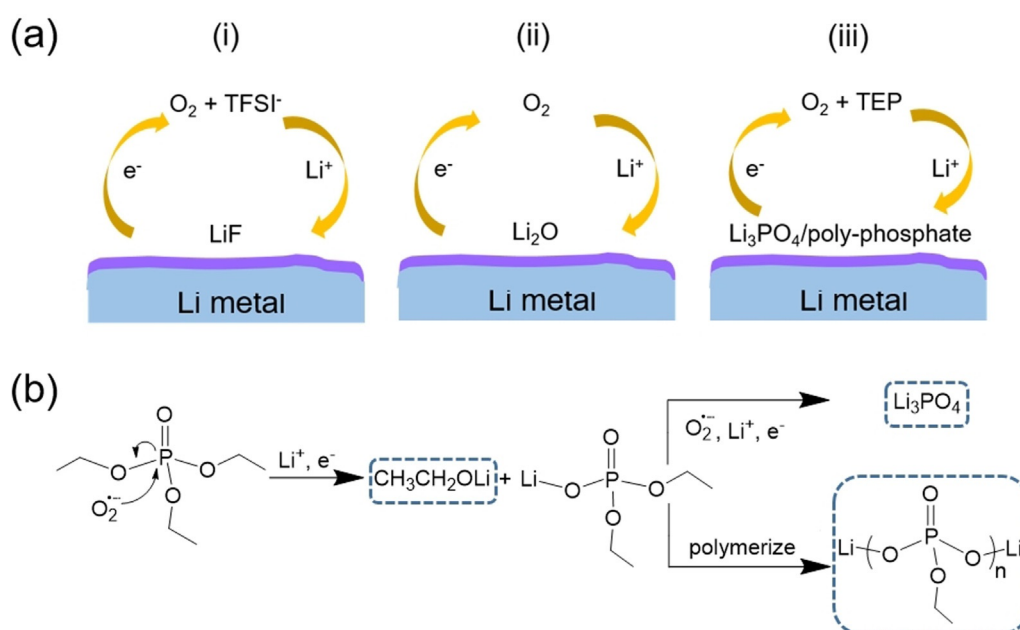
Figure 3. a) Possible chemical/electrochemical reactions in TEP electrolyte; b) Proposed reaction pathways toward the formation of Li_3PO_4/poly-phosphates SEI on Li metal surface.

plating.[20–23] These approaches are based on the premise that the electrolyte decomposition could produce LiF-rich SEIs that are beneficial for Li stripping/plating. To measure the compositions of the SEI, we collected X-ray photoelectron spectra (XPS) on the Cu working electrode after Li plating. No measurable increase of LiF contents was observed (Figure S7a). Given that the TFSI$^-$ concentration is relatively low (1 M), the first possibility of TFSI$^-$ decomposition as the main reason for the dramatic increase of the cycling performance is highly unlikely. To further support this conclusion, we conducted similar cycling experiments as those shown in Figure 1c but with 1 M $LiClO_4$ (in TEP) as the support electrolyte and observed similar results (Figure S8a). Taken together, the evidence clearly ruled out the first possibility as shown in Figure 3a.

The second possibility of Li_2O formation on the anode was next considered. Given the presence of O_2 and the low electrochemical potentials of Li oxidation, it is conceivable that Li_2O may form on the anode. Recent studies have shown that Li_2O could play a positive role as a component in the SEI formed in ether-based electrolytes.[37,38] To test this possibility, we carried out control experiments to pre-form Li_2O via treating Li foil with dry O_2. XPS studies confirmed that this treatment indeed increased O content on the surface (Figure S9a). Afterwards, the treated Li foil was used as the working electrode in a symmetric Li∥Li cell for cycling test. Without O_2 in the TEP electrolyte, the cell failed within 6 cycles (Figure S10a). This set of experiments suggest that ex situ formed Li_2O does not enable Li stripping/plating in TEP. One may argue that in situ formed Li_2O by electrochemistry is necessary for the purpose. To address this concern, we employed the second method of promoting Li_2O formation in a Li∥Li cell in an ether-based electrolyte (1 M LiTFSI in tetraethylene glycol dimethyl ether (TEGDME)). After

5 cycles of repeated stripping and plating, a Li_2O-rich SEI was confirmed by XPS on Li surface (Figure S9b). The Li foil was then removed from the first cell and washed with 1,2-dimethoxyethane (DME). A new test cell was assembled with TEP as the support electrolyte. Without O_2, the cell failed quickly after 7 cycles, too (Figure S10b). Taken together, we concluded that the reaction between O_2 and Li cannot account for the observed improvement.

With the first two possibilities excluded, we are now guided to understand the improvement as a result of the unique reactions between TEP solvent and reactive O_2 species under electrochemical conditions. Close examinations of Figure 1a reveal that O_2 is reduced at potentials < 2.2 V during the first cycle. As the most likely species of the first electron transfer during oxygen reduction reaction (ORR) in an aprotic electrolyte, $O_2^{\cdot-}$ is a nucleophile.[39] It can substitute the ethoxy group of TEP via the SN2 mechanism or abstract the neighboring hydrogen atom, as has been reported in the literature.[40,41] Subsequent electron transfer and O–O bond dissociation are expected to lead to the production of Li_3PO_4 or other poly-phosphates products. The two hypothesized reaction pathways are illustrated schematically in Figure 3b and Figures S11-12. We first took advantage of theoretical calculations to investigate the two possible reaction pathways. DFT calculation results suggest that both reaction pathways are thermodynamically favorable. For Pathway **I**, it was found that the initial reactions actually would follow the addition-elimination mechanism rather than direct SN2 substitution. This preference of the addition-elimination mechanism over the direct SN2 mechanism has been proposed and tested experimentally for trivalent phosphorus before.[42] The rate-limiting step (RLS) of Pathway **I** is the leaving of the ethoxide groups (Figure 4a and Table S2). For Pathway **II**, it was found that the RLS could be the abstracting of H atom or cleavage
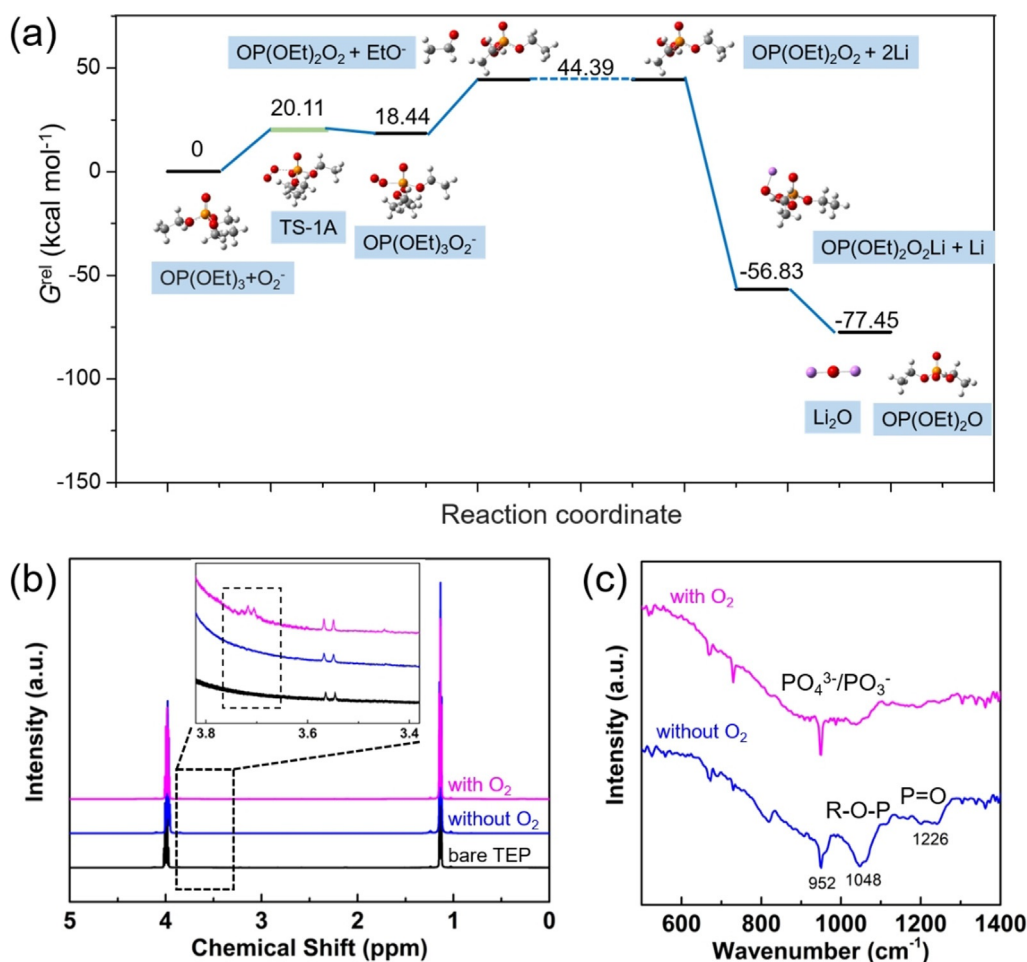
Figure 4. a) The relative free energy G^{rel} scheme for the hypothetical reaction Pathway **I** computed by the M06-2X functional; b) NMR spectra of TEP electrolytes after cycling Li‖Li cells with or without O_2; c) IR spectra of deposited Li on Cu substrate surfaces in cells with or without O_2.

of O−O bond, both of which feature energy barriers nearly twice as high as those in Pathway **I** (Figure S13 and Table S3). If these mechanisms held true, we would expect the release of Li ethoxide (CH_3CH_2OLi) as a by-product of Pathway **I** or the formation of Li acetate (CH_3COOLi) from Pathway **II**. Indeed, 1H nuclear magnetic resonance (NMR) spectra clearly confirmed this expectation. By analyzing the electrolyte solutions after cycling in Li‖Li cells, we identified the peak at 3.71 ppm chemical shift to correspond to H in CH_3-**CH_2**-O-Li (Figure 4b).[43] The experimental evidence supports that Pathway **I** is more likely, consistent with the understanding inferred from DFT calculations. It is worth noting that we also calculated the NMR chemical shifts of CH_3CH_2OLi, and the result was in good agreement of our measured values (Figure S14). We next studied the SEI by Fourier-transform infrared spectroscopy (FTIR). It is observed in Figure 4c that the introduction of O_2 clearly suppressed the formation of chemicals that give rise to IR peaks at 1048 and 1226 cm^{-1}. According to the literature,[44–46] they correspond to the stretching of ester group (P-O-R) and P=O, respectively, in organo-phosphorous species. The distinct peak at 952 cm^{-1} reports on the P-O stretching in ortho-phosphates (PO_4^{3-}) or meta-phosphates (PO_3^-). This set of data suggests that direct TEP decomposition produces

organo-phosphorous species; the introduction of O_2 alters the reaction pathways to promote the formation of Li_3PO_4/poly-phosphates.

It has been reported that Li-conducting Li_3PO_4 SEI layer with a high Young's modulus can effectively suppress side reactions between Li and the electrolyte and thus limit Li dendrite growth.[47–49] Moreover, a layer of cross-linked poly-phosphates is expected to prevent direct decomposition of TEP and buffer the volume change during Li stripping/plating, in a similar fashion to how poly-carbonates in the SEI enable the operation of graphite electrode.[50,51] We are, therefore, inspired to understand the effects as follows. Electrochemically reduced O_2 leads to the unique decomposition of TEP to yield a thin layer of SEI rich in Li_3PO_4 and poly-phosphates. Such an SEI exhibits desired electrical and mechanical properties to regulate Li plating. The net result is that the plated Li is dense and free of dendrites. The stark difference of the plated Li for TEP with and without O_2 (Figure 2) strongly supports this hypothesis. To further validate the conjecture, we performed electrochemical characterization by electrochemical impedance spectroscopy (EIS). Here, a Li‖Li cell was examined as a function of the cycling history. It is seen in Figure S15 that the initial charge transfer resistance was similar for cells with or without O_2 (ca.

300 Ω). After only 1 cycle of Li stripping/plating, the resistance increased dramatically (to ca. 1900 Ω) for the cell without O_2; in stark contrast, that for the cell with O_2 did not change significantly. The comparison highlights that direct decomposition of TEP under electrochemical conditions is highly detrimental to Li stripping/plating, consistent with prior reports that organo-lithium compounds (e.g. lithiated phosphates) and inorganic lithium salts (e.g. LiOH) are poor Li^+ conductors.[28,52] In fact, the measured resistance would increase to ca. 2700 Ω after 10 cycles for a cell without O_2, making it meaningless to further characterize the cell. The increase of the charge transfer resistance as measured by EIS agrees with the rapid rise of the overpotentials as shown in Figure 1c. By comparison, repeated stripping/plating of Li in TEP with O_2 gradually decreased the charge transfer resistance to ca. 220 Ω after 40 cycles. Of course, we are mindful that the resistance is still too high for practical applications, and further research will be needed to further reduce the contact resistance. The results are encouraging, nonetheless, as they are comparable with other literature reports studying Li metal as an anode, particularly in non-flammable phosphate electrolytes.[35,53] Most encouragingly, the nature of the reaction is such that the resistance actually decreases over cycling, strongly suggesting that a favorable SEI is formed, as is true in other functional SEI formation processes. To the best of our knowledge, this is the first time that a unique electrochemically induced electrolyte decomposition pathway is proposed. The mechanism not only

enriches the knowledge on the complex reactions that enable the formation of a "good" SEI, but also serves as a facile approach to enable the utilization of an otherwise difficult to implement electrolyte. Next, we explored the utility of the as-formed SEI in protecting Li metal as an anode in Li-O_2 and Li-ion batteries.

Given the involvement of O_2 in the above-identified processes, the first prototypical battery we sought to test was Li-O_2 batteries with TEP as an electrolyte. Due to the poor performance of the anode, earlier attempts toward this end have concluded that organic phosphate-based electrolytes was not compatible with Li-O_2 batteries.[41,54] To prove that the system indeed works, we first studied the electrochemical behaviors of the system in a three-electrode configuration, where glassy carbon was used as the working electrode, and two Li ribbons were used as the counter and reference electrodes. As shown in Figure 5a, the reduction wave took off at ca. 2.6 V, corresponding to the $O_2 \rightarrow Li_2O_2$ reaction; on the reverse scan, the oxidation wave was observed starting from ca. 3.0 V, corresponding to the O_2 evolution reaction. The redox features in TEP electrolyte resembled those in ether-based electrolytes, which are well established for Li-O_2 battery operations.[55,56] Importantly, these electrochemical features were absent without O_2, strongly suggesting that they report on reversible O_2 reduction and evolution in a TEP electrolyte, which is desired but has not been reported previously. Then we fabricated a Li-O_2 full cell for galvanostatic tests. Three dimensionally ordered mesoporous carbon
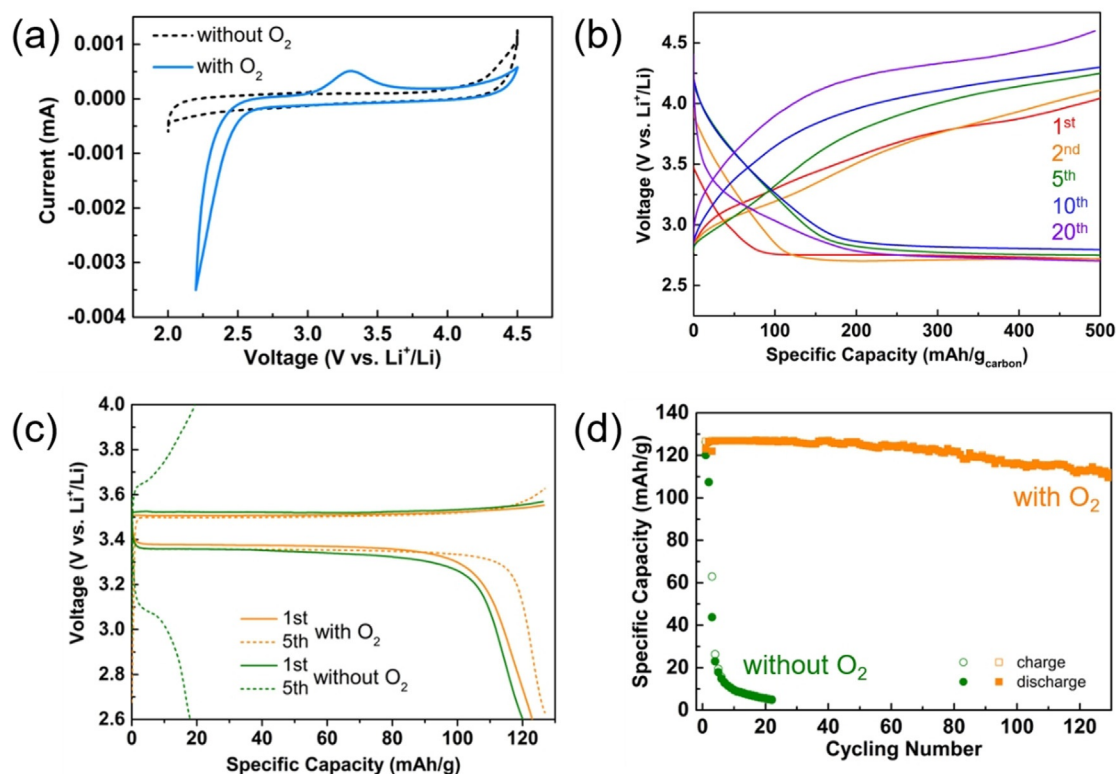
Figure 5. Prototype Li-O_2 cell and Li-ion cell test in TEP electrolyte. a) CV studies in a three-electrode system (WE: glassy carbon, CE: Li strip, RE: Li strip) with or without O_2; b) Charge-discharge profile of the Li-O_2 cell with 3DOm carbon as cathode (cycling under constant current (100 mA g_{carbon}^{-1}) with a cut-off capacity of 500 mAh g_{carbon}^{-1}); c) Charge-discharge profile and d) Cycling performance of the Li ∥ LFP cells with or without O_2 at a current density of 0.2 C.

(3DOm) was used as the cathode to take advantage of its good performance for such applications, especially its stability against oxidation.[57] As shown Figure 5b, more than 20 cycles of discharge and recharge were achieved at a current density of 100 mA/g_{carbon} in TEP electrolyte with the charge potential cut-off as 4.5 V. The cycling performance is comparable to that in the more popularly studied 1,2-dimethoxyethane (DME) electrolyte under similar test conditions.[57] To confirm that the electrochemical features indeed report on the formation and decomposition of Li_2O_2 as the main discharge product, the morphology of deep-discharged cathode was studied by SEM. Figure S17a shows that a representative toroidal structure was observed, consistent with literature reports where fast kinetics favors toroid formation.[58] The Raman spectra in Figure S17b also proved Li_2O_2 as the discharge product.[59] It is worth highlighting that the results were obtained by using Li metal as the anode without special protections. This is the first time that a non-flammable phosphate electrolyte is demonstrated for the operation of Li-O_2 batteries. It opens up the door to constructing safe Li-O_2 batteries that could offer high energy densities to fully actualize the potentials held by this new chemistry.

With encouraging results on Li-O_2 batteries established, we next tested whether the same strategy works for Li-ion batteries. For this purpose, a full battery consisting of LiFePO$_4$ (LFP) as the cathode and a Li metal as the anode was fabricated. Stark differences were readily observed in the voltage-capacity profiles as shown in Figure 5c with and without O_2. The presence of O_2 promoted the formation of functional SEI on the Li anode and established stable charge and discharge plateaus at 3.50 V and 3.35 V, respectively.[60] In contrast, no stable charge/discharge plateau was observed in the cell without O_2 after 5 cycles, which quickly worsened even further afterwards because of the increasing overpotential on the Li anode side. Subsequent cycling tests of the cell (Figure 5d) exhibits more than 130 reversible cycles with capacity retention of 82% by introducing O_2 as additives. The cell without O_2 exhibits very low efficiency and capacity because TEP is incompatible to Li metal anode. These experiments further demonstrate that our strategy can be utilized to promote the development of Li metal anode in Li-ion batteries and make nonflammable TEP electrolyte as a promising candidate.

Conclusion

In conclusion, we have demonstrated that O_2 as an additive can enable Li metal anode operations in a nonflammable TEP-based electrolyte. The mechanism involves induced TEP decomposition by electrochemically reduced O_2, which produces a favorable SEI layer to support repeated Li stripping/plating. The SEI not only suppresses Li dendrite formation, but also limits further TEP decomposition. Given the nonflammable nature of TEP, this system promises safe operations of Li metal as an anode. To this end, the potentials are demonstrated in a Li-O_2 and a Li-ion prototypical battery. While further optimization (e.g., further improvement of the Coulombic Efficiencies) will likely be necessary to make the

strategy practice for battery applications, this body of work provides a new understanding on the mechanism by which SEI forms on Li metal anode, which will likely benefit the development of future high energy density battery technologies.

Conflict of interest

The authors declare no conflict of interest.

[1] D. H. Doughty, E. P. Roth, *Electrochem. Soc. Interface* **2012**, *21*, 37.

[2] K. Liu, Y. Liu, D. Lin, A. Pei, Y. Cui, *Sci. Adv.* **2018**, *4*, eaas9820.

[3] C. Uhlmann, J. Illig, M. Ender, R. Schuster, E. Ivers-Tiffée, *J. Power Sources* **2015**, *279*, 428–438.

[4] T. Waldmann, B.-I. Hogg, M. Wohlfahrt-Mehrens, *J. Power Sources* **2018**, *384*, 107–124.

[5] E. J. McShane, A. M. Colclasure, D. E. Brown, Z. M. Konz, K. Smith, B. D. McCloskey, *ACS Energy Lett.* **2020**, *5*, 2045–2051.

[6] S. J. An, J. Li, C. Daniel, D. Mohanty, S. Nagpure, D. L. Wood, *Carbon* **2016**, *105*, 52–76.

[7] X.-B. Cheng, R. Zhang, C.-Z. Zhao, Q. Zhang, *Chem. Rev.* **2017**, *117*, 10403–10473.

[8] D. Aurbach, A. Zaban, A. Schechter, Y. Ein-Eli, E. Zinigrad, B. Markovsky, *J. Electrochem. Soc.* **1995**, *142*, 2873.

[9] D. Aurbach, B. Markovsky, A. Shechter, Y. Ein-Eli, H. Cohen, *J. Electrochem. Soc.* **1996**, *143*, 3809.

[10] Y. Zhang, Y. Zhong, Q. Shi, S. Liang, H. Wang, *J. Phys. Chem. C* **2018**, *122*, 21462–21467.

[11] D. Lin, Y. Liu, Y. Cui, *Nat. Nanotechnol.* **2017**, *12*, 194–206.

[12] B. Liu, J.-G. Zhang, W. Xu, *Joule* **2018**, *2*, 833–845.

[13] C. Fang, X. Wang, Y. S. Meng, *Trends Chem.* **2019**, *1*, 152–158.

[14] A. Markevich, G. Salitra, F. Chesneau, M. Schmidt, D. Aurbach, *ACS Energy Lett.* **2017**, *2*, 1321–1326.

[15] Z. L. Brown, S. Jurng, C. C. Nguyen, B. L. Lucht, *ACS Appl. Energy Mater.* **2018**, *1*, 3057–3062.

[16] T. Li, X.-Q. Zhang, P. Shi, Q. Zhang, *Joule* **2019**, *3*, 2647–2661.

[17] Y. Liu, D. Lin, Y. Li, G. Chen, A. Pei, O. Nix, Y. Li, Y. Cui, *Nat. Commun.* **2018**, *9*, 3656.

[18] C. Yan, Y.-X. Yao, X. Chen, X.-B. Cheng, X.-Q. Zhang, J.-Q. Huang, Q. Zhang, *Angew. Chem. Int. Ed.* **2018**, *57*, 14055–14059; *Angew. Chem.* **2018**, *130*, 14251–14255.

[19] Y. Gao, Z. Yan, J. L. Gray, X. He, D. Wang, T. Chen, Q. Huang, Y. C. Li, H. Wang, S. H. Kim, T. E. Mallouk, D. Wang, *Nat. Mater.* **2019**, *18*, 384–389.

[20] J. Wang, Y. Yamada, K. Sodeyama, E. Watanabe, K. Takada, Y. Tateyama, A. Yamada, *Nat. Energy* **2018**, *3*, 22–29.

[21] Z. Zeng, V. Murugesan, K. S. Han, X. Jiang, Y. Cao, L. Xiao, X. Ai, H. Yang, J.-G. Zhang, M. L. Sushko, J. Liu, *Nat. Energy* **2018**, *3*, 674–681.

[22] L. Suo, Y.-S. Hu, H. Li, M. Armand, L. Chen, *Nat. Commun.* **2013**, *4*, 1481.

[23] X. Fan, L. Chen, X. Ji, T. Deng, S. Hou, J. Chen, J. Zheng, F. Wang, J. Jiang, K. Xu, C. Wang, *Chem* **2018**, *4*, 174–185.

[24] X. Fan, L. Chen, O. Borodin, X. Ji, J. Chen, S. Hou, T. Deng, J. Zheng, C. Yang, S.-C. Liou, K. Amine, K. Xu, C. Wang, *Nat. Nanotechnol.* **2018**, *13*, 715–722.

[25] Z. Yu, H. Wang, X. Kong, W. Huang, Y. Tsao, D. G. Mackanic, K. Wang, X. Wang, W. Huang, S. Choudhury, Y. Zheng, C. V. Amanchukwu, S. T. Hung, Y. Ma, E. G. Lomeli, J. Qin, Y. Cui, Z. Bao, *Nat. Energy* **2020**, *5*, 526–533.

[26] X. Wang, E. Yasukawa, S. Kasuya, *J. Electrochem. Soc.* **2001**, *148*, A1058–A1065.

[27] K. Xu, M. S. Ding, S. Zhang, J. L. Allen, T. R. Jow, *J. Electrochem. Soc.* **2003**, *150*, A161–A169.

[28] X. Wang, E. Yasukawa, S. Kasuya, *J. Electrochem. Soc.* **2001**, *148*, A1066–A1071.

[29] K. Xu, S. Zhang, J. L. Allen, T. R. Jow, *J. Electrochem. Soc.* **2003**, *150*, A170–A175.

[30] S.-J. Tan, J. Yue, X.-C. Hu, Z.-Z. Shen, W.-P. Wang, J.-Y. Li, T.-T. Zuo, H. Duan, Y. Xiao, Y.-X. Yin, R. Wen, Y.-G. Guo, *Angew. Chem. Int. Ed.* **2019**, *58*, 7802–7807; *Angew. Chem.* **2019**, *131*, 7884–7889.

[31] S. Chen, J. Zheng, L. Yu, X. Ren, M. H. Engelhard, C. Niu, H. Lee, W. Xu, J. Xiao, J. Liu, J.-G. Zhang, *Joule* **2018**, *2*, 1548–1558.

[32] T. Liu, L. Lin, X. Bi, L. Tian, K. Yang, J. Liu, M. Li, Z. Chen, J. Lu, K. Amine, K. Xu, F. Pan, *Nat. Nanotechnol.* **2019**, *14*, 50–56.

[33] B. D. Adams, J. Zheng, X. Ren, W. Xu, J.-G. Zhang, *Adv. Energy Mater.* **2018**, *8*, 1702097.

[34] R. S. Assary, J. Lu, P. Du, X. Luo, X. Zhang, Y. Ren, L. A. Curtiss, K. Amine, *ChemSusChem* **2013**, *6*, 51–55.

[35] L. Xiao, Z. Zeng, X. Liu, Y. Fang, X. Jiang, Y. Shao, L. Zhuang, X. Ai, H. Yang, Y. Cao, J. Liu, *ACS Energy Lett.* **2019**, *4*, 483–488.

[36] C. Fang, J. Li, M. Zhang, Y. Zhang, F. Yang, J. Z. Lee, M.-H. Lee, J. Alvarado, M. A. Schroeder, Y. Yang, B. Lu, N. Williams, M. Ceja, L. Yang, M. Cai, J. Gu, K. Xu, X. Wang, Y. S. Meng, *Nature* **2019**, *572*, 511–515.

[37] F. Qiu, X. Zhang, Y. Qiao, X. Zhang, H. Deng, T. Shi, P. He, H. Zhou, *Energy Storage Mater.* **2018**, *12*, 176–182.

[38] E. Wang, S. Dey, T. Liu, S. Menkin, C. P. Grey, *ACS Energy Lett.* **2020**, *5*, 1088–1094.

[39] X. Yao, Q. Dong, Q. Cheng, D. Wang, *Angew. Chem. Int. Ed.* **2016**, *55*, 11344–11353; *Angew. Chem.* **2016**, *128*, 11514–11524.

[40] D. C. Isbell, R. R. Dewald, *J. Phys. Chem.* **1987**, *91*, 6695–6698.

[41] Z. E. M. Reeve, A. D. Pauric, K. J. Harris, G. R. Goward, *J. Phys. Chem. C* **2015**, *119*, 26840–26848.

[42] J. Li, P. Beak, *J. Am. Chem. Soc.* **1992**, *114*, 9206–9207.

[43] G. García-Herbosa, M. Aparicio, J. Mosa, J. V. Cuevas, T. Torroba, *Dalton Trans.* **2016**, *45*, 13888–13898.

[44] L. Daasch, D. Smith, *Anal. Chem.* **1951**, *23*, 853–868.

[45] L. Popović, D. de Waal, J. C. A. Boeyens, *J. Raman Spectrosc.* **2005**, *36*, 2–11.

[46] A. H. Ahmad, A. K. Arof, *Ionics* **2004**, *10*, 200–205.

[47] N.-W. Li, Y.-X. Yin, C.-P. Yang, Y.-G. Guo, *Adv. Mater.* **2016**, *28*, 1853–1858.

[48] L. Wang, Q. Wang, W. Jia, S. Chen, P. Gao, J. Li, *J. Power Sources* **2017**, *342*, 175–182.

[49] K.-E. Kim, J. Y. Jang, I. Park, M.-H. Woo, M.-H. Jeong, W. C. Shin, M. Ue, N.-S. Choi, *Electrochem. Commun.* **2015**, *61*, 121–124.

[50] C. C. Nguyen, B. L. Lucht, *J. Electrochem. Soc.* **2014**, *161*, A1933.

[51] M. Nie, J. Demeaux, B. T. Young, D. R. Heskett, Y. Chen, A. Bose, J. C. Woicik, B. L. Lucht, *J. Electrochem. Soc.* **2015**, *162*, A7008.

[52] N. Feng, P. He, H. Zhou, *Adv. Energy Mater.* **2016**, *6*, 1502303.

[53] Y. Dong, N. Zhang, C. Li, Y. Zhang, M. Jia, Y. Wang, Y. Zhao, L. Jiao, F. Cheng, J. Xu, *ACS Appl. Energy Mater.* **2019**, *2*, 2708–2716.

[54] W. Xu, J. Hu, M. H. Engelhard, S. A. Towne, J. S. Hardy, J. Xiao, J. Feng, M. Y. Hu, J. Zhang, F. Ding, M. E. Gross, J.-G. Zhang, *J. Power Sources* **2012**, *215*, 240–247.

[55] Y.-C. Lu, B. M. Gallant, D. G. Kwabi, J. R. Harding, R. R. Mitchell, M. S. Whittingham, Y. Shao-Horn, *Energy Environ. Sci.* **2013**, *6*, 750–768.

[56] F. Li, D.-M. Tang, Y. Chen, D. Golberg, H. Kitaura, T. Zhang, A. Yamada, H. Zhou, *Nano Lett.* **2013**, *13*, 4702–4707.

[57] J. Xie, X. Yao, Q. Cheng, I. P. Madden, P. Dornath, C.-C. Chang, W. Fan, D. Wang, *Angew. Chem. Int. Ed.* **2015**, *54*, 4299–4303; *Angew. Chem.* **2015**, *127*, 4373–4377.

[58] N. B. Aetukuri, B. D. McCloskey, J. M. García, L. E. Krupp, V. Viswanathan, A. C. Luntz, *Nat. Chem.* **2015**, *7*, 50–56.

[59] D. Zhai, H.-H. Wang, K. C. Lau, J. Gao, P. C. Redfern, F. Kang, B. Li, E. Indacochea, U. Das, H.-H. Sun, H.-J. Sun, K. Amine, L. A. Curtiss, *J. Phys. Chem. Lett.* **2014**, *5*, 2705–2710.

[60] L.-X. Yuan, Z.-H. Wang, W.-X. Zhang, X.-L. Hu, J.-T. Chen, Y.-H. Huang, J. B. Goodenough, *Energy Environ. Sci.* **2011**, *4*, 269–284.